Cellular Signalling 53 (2019) 224–233

Contents lists available at ScienceDirect

Cellular Signalling

journal homepage: www.elsevier.com/locate/cellsig

Chemical denervation using botulinum toxin increases Akt expression and reduces submaximal insulin-stimulated glucose transport in mouse muscle

Zhencheng Li[a,1], Lui Näslund-Koch[a,b,1], Carlos Henriquez-Olguin[a], Jonas R. Knudsen[a], Jingwen Li[a], Agnete B. Madsen[a], Satoru Ato[d], Jacob Wienecke[c], Riki Ogasawara[d], Jens B. Nielsen[b], Thomas E. Jensen[a,*]

[a] Section of Molecular Physiology, Department of Nutrition, Exercise and Sports, University of Copenhagen, Denmark
[b] Neural Control of Movement Research Group, Department of Neuroscience, University of Copenhagen, Copenhagen, Denmark
[c] Section of Integrated Physiology, Department of Nutrition, Exercise and Sports, University of Copenhagen, Denmark
[d] Nagoya Institute of Technology, Nagoya, Japan

ARTICLE INFO

Keywords:
Atrophy
GLUT4
Hexokinase
TBC1D4
Insulin signaling

ABSTRACT

Botulinum toxin A (botox) is a toxin used for spasticity treatment and cosmetic purposes. Botox blocks the excitation of skeletal muscle fibers by preventing the release of acetylcholine from motor nerves, a process termed chemical denervation. Surgical denervation is associated with increased expression of the canonical insulin-activated kinase Akt, lower expression of glucose handling proteins GLUT4 and hexokinase II (HKII) and insulin resistant glucose uptake, but it is not known if botox has a similar effect. To test this, we performed a time-course study using supra-maximal insulin-stimulation in mouse soleus ex vivo. No effect was observed in the glucose transport responsiveness at day 1, 7 and 21 after intramuscular botox injection, despite lower expression of GLUT4, HKII and expression and phosphorylation of TBC1D4. Akt protein expression and phosphorylation of the upstream kinase Akt were increased by botox treatment at day 21. In a follow-up study, botox decreased submaximal insulin-stimulated glucose transport. The marked alterations of insulin signaling, GLUT4 and HKII and submaximal insulin-stimulated glucose transport are a potential concern with botox treatment which merit further investigation in human muscle. Furthermore, the botox-induced chemical denervation model may be a less invasive alternative to surgical denervation.

1. Introduction

Since the late 1980's, botulinum toxin A (botox) has become widely used in the treatment of spasticity and in the cosmetic industry [1,2]. Botox is a toxin produced by the bacterium clostridium botulinum which blocks the release of acetylcholine from the nerve ending of the motor neuron. It does so by cleaving the SNARE protein, SNAP-25, which plays a role in the docking and fusion of acetylcholine-vesicles at the surface membrane, thereby suppressing neurotransmission and preventing muscle contraction [3–5]. When injecting botox into skeletal muscle, a dose-dependent decrease of neurotransmitter exocytosis, termed chemical denervation is observed [6].

The general consensus is that the use of botox is safe, efficient and without serious side-effects in human patients [7]. However, more invasive and detailed studies in rodents suggest that botox injection causes marked disruption of skeletal muscle tissue architecture, with e.g. increased collagen turnover and inflammation [8,9]. Furthermore, in relation to glucose metabolism, various acute models of rodent muscle hind limb denervation have reported impaired insulin-stimulated glucose uptake into muscle [10–14]. Chronically, rodent surgical denervation of skeletal muscle has repeatedly been shown to decrease the mRNA expression of the insulin-responsive glucose transporter 4 (GLUT4), with a more variable effect on protein expression [15–18]. In contrast, the classical insulin-activated and glucose uptake-regulating kinase Akt2 was reported to increase with surgical denervation both at the protein expression and phosphorylation level [16,19,20].

It is currently undetermined if treatment of muscle spasticity with botox affects metabolic regulation. Furthermore, chemical denervation using botox might be a useful and minimally invasive research model in which to study denervation-induced changes in skeletal muscle size and function. We therefore conducted a botox denervation time course study in mice a) to explore the utility of the botox denervation model as

* Corresponding author.
E-mail address: tejensen@nexs.ku.dk (T.E. Jensen).
[1] Denotes equal contribution.

https://doi.org/10.1016/j.cellsig.2018.10.014
Received 25 June 2018; Received in revised form 17 October 2018; Accepted 19 October 2018
Available online 21 October 2018
0898-6568/

such and b) to specifically investigate the impact of botox denervation on insulin-regulated Akt signaling, glucose uptake and glucose handling proteins.

2. Materials and methods

2.1. Animals

All experiments were approved by the Danish Animal Experimental Inspectorate and complied with the European Convention for the Protection of Vertebrate Animals Used for Experiments and Other Scientific Purposes. Female C57BL/6 mice (Taconic, Lille Skensved, Denmark), aged 12–16 weeks, were used for all experiments. The animals were maintained on a 12:12-h light-dark cycle and received standard rodent diet and water ad libitum for at least one week before experiments.

2.2. Botox injection procedure

Mice were anesthetized with ketamine/xylazine (20% of 100 mg/ml; 10% of 20 mg/ml respectively, 0.1 ml/10 g). While anesthetized, both hind limbs were shaved. Intramuscular (IM) injections of 0.5 U of botox were performed through the skin based on previous publications in mice [21–23]. Botox (Allergan Inc. Irvine CA) in 50-unit (U) vials was dissolved according to the manufacturer's instructions, with 2 ml 0.9% sodium chloride, resulting in a concentration of 2.5 U/100 µl [24]. The soleus (SOL) and surrounding gastrocnemius muscle was injected with botox or saline at the median of the dorsal side of the lower leg approximately 5 mm distal of the knee joint in a ~40° angle, pointing the needle distally. The tibialis anterior (TA) muscles were injected at a ~45° angle with the needle pointing medial distally on the lateral side of the leg approximately 3–5 mm beneath the knee joint [25]. All botox injections were performed in the right hind limb with saline control injections in the opposite leg. To control for botox spillover to non-injected muscles and compensatory use of the contralateral leg, a separate group of mice received saline injections in both legs. Injections were made in a fixed volume of 20 µl using a sterile 30G needle attached to a 300 µl syringe, at day 0 [24,26]. In the 7-day follow-up experiment, the mice were injected with 0.5 U in the triceps surae only. Only the SOL muscle was used for muscle incubation in the present study due to its enriched expression of TBC1D4 [27].

2.3. Muscle incubation

The mice were sacrificed at day 1, 7 or 21. SOL muscles were obtained from anesthetized mice (90% pentobarbital (50 mg/ml) and 10% xylocaine (20 mg/ml) 100 g^{-1} body weight) and immediately pinned with needles on custom-made plastic holders at their approximate resting length in borosilicate glass culture tubes, 16 × 100 mm, 15 ml (Kimble, Rockwood, USA) [28,29]. They were then pre-incubated for 30 min in 3 ml Krebs-Ringer-Henseleit (KRH) buffer supplemented with 2 mM pyruvate, and 8 mM mannitol. The incubations were performed at 30 °C in a water bath, and the buffers were gassed with 95% O_2–5% CO_2 [28–30]. All reagents used for incubation and biochemical analyses were from Sigma-Aldrich unless otherwise stated. The holders with muscles were then transferred to new tubes for 10 min ± insulin (dose: 60 nM, Actrapid®, Novo Nordisk, Denmark) followed by transferring to new tubes for 10 min + 2-deoxy-D-glucose (2DG) tracer to measure 2DG transport ± insulin. The 2DG tracer medium contained 2-[2,6-^{3}H] deoxy-D-glucose (1 mM) and [1-^{14}C] mannitol (8 mM) (Amersham Biosciences; specific activities of the two tracers in the medium were 0.12 and 0.11 µCi ml^{-1}, respectively). Lastly, the muscles were washed in ice-cold KRH buffer, blotted dry and snap-frozen in liquid nitrogen, trimmed and weighed in the frozen state before being stored at −80 °C until further processing.

In the follow-up experiment examining submaximal insulin-stimulation, 3 groups of mice were injected in the gastrocnemius at day 0 with saline or botox, or at day 6 with botox. Body weight and food intake was monitored throughout. On day 7, the same ex vivo incubation procedure as above was followed with the exception of drawing a blood sample post-mortem for evaluation of fasting glucose and insulin, the use of a submaximal 1.5 nM insulin-dose and the post-mortem embedding of gastrocnemius muscle to determine fiber cross sectional area. HOMA2-IR was calculated as previously described [31].

2.4. 2-Deoxyglucose (2DG) transport

Glucose transport was determined from the intracellular accumulation of non-metabolizable 2-[^{3}H]deoxy-D-glucose [32] using D-[1-^{14}C] mannitol to estimate the extracellular space. For analysis of glucose transport, 100 of 300 µl muscle lysate were mixed with 2 ml of Ultima Gold™ scintillation cocktail (Perkin Elmer, MA, USA). 100 µl of double distilled water and 50 µl of tracer medium were added to similar tubes in duplicates, to subtract background activity and estimate the specific activity in the medium. Tubes were vigorously shaken and radioactivity was measured using liquid scintillation counting (Tri-Carb 2000; Packard Instrument, Downers Grove, IL) [32,33].

2.5. Muscle analysis

Muscles were homogenized in ice-cold lysis buffer (300 µl/muscle; 50 mM Tris base, 150 mM NaCl, 1 mM ethylene-diamin-tetraacetic-acid, 1 mM ethylene-glycol-tetraacetic-acid, 2 mM sodium orthovanadate, 1 mM dithiothreitol (DTT), 50 mM sodium fluoride, 5 mM sodium pyrophosphate, 1 mM benzamidine, 0.5% Protease inhibitor cocktail (PIC; Sigma P8340), 20% NP-40, pH 7.4) lysed using a bead mill at 30 Hz for 1 min (Tissue Lyser II -Qiagen). The homogenates were rotated end over end for 30 min at 4 °C. Lysates were generated by centrifugation (Universal 320R, Hettich Zentrifugen) at 18.320 G for 20 min at 4 °C. The pellet was discarded and the supernatant stored at −80 °C for further analyses.

2.6. Immunoblotting

Lysate protein concentration was measured using the bicinchoninic acid method in triplicate using known concentrations of BSA as standards (Pierce, Rockford, IL, USA). To determine total and phosphorylated levels of relevant proteins, equal amounts of protein were electrophoresed on 5–16% self-cast SDS-PAGE gels (Biorad mini-PROTEAN) and transferred by semidry blotting to polyvindylidenedifluoride (PVDF) membranes (Immobilon Transfer Membrane; Millipore, Copenhagen, Denmark). The primary antibodies used were phospho-p38 MAPK Thr180/Tyr182 (Cell Signaling Technology (CST), 9211), phospho-Akt Thr308 (CST, 13038), phospho-Akt Ser473 (CST, 4060), phospho-TBC1D4 Thr642 (CST, 8881), phospho-ACC Ser212 (Millipore, 03303), Akt2 (CST, 2964), Hexokinase II (HKII) (CST, 2867), TBC1D4 (CST, 2447), GLUT4 (ThermoFisher Scientific, PA5–23052) and ACC1/2 (DAKO DENMARK, P0397).

The blotted PVDF membranes were blocked for 30 min in Tris-buffered saline-Tween 20 (TBS-T) plus 3% skimmed milk powder at room temperature and incubated with primary antibodies overnight at 4^{0}C, followed by three brief washes in TBS-T before incubation with horseradish peroxidase-conjugated secondary antibody (Jackson, Maine, USA) for 45 min at room temperature. Bands were visualized using a ChemiDoc MP Imaging System (Bio-Rad, Hercules, CA, USA) and quantified using Image Lab Version 5.2.1 for PC (Bio-Rad software). Coomassie staining of developed blots was used to validate even transfer and quasi-equal loading of protein.

2.7. Fiber size analysis

Botox and saline-treated gastrocnemius muscles (n = 5) were

embedded in tissue-tek, frozen in liquid nitrogen-cooled isopentane and stored at −80 °C. Frozen muscle was transferred to a cryostat chamber and allowed to equilibrate to −25 °C. Transverse sections of 10 μm were cut and mounted on positively charged glass slides (Thermo Fisher Scientific). Samples were fixed in 2% paraformaldehyde for 10 min, followed by three washes in phosphate-buffered saline (PBS). Oregon green-conjugated wheat germ agglutinin (WGA) (1:200) was used to stain the basal lamina. Images were collected using a LSM710 confocal microscope (Carl Zeiss, Oberkochen, Germany) with a 40 × 1.3 NA objective lens. For quantification of fiber size, cross-sectional area measurements were performed using the particle size tool in ImageJ (National Institute of Health). Five areas in 1 mid muscle-belly cryosection were counted, on average > 50 fibers/area All image collections and quantifications were performed blinded.

2.8. RT-qPCR analysis

The qPCR workflow was carried as described previously [34] with the following modifications: RNA extraction was performed using ISOGEN II (Nippon Gene, Tokyo, Japan), in accordance with the manufacturer's instructions, total RNA measurement was performed using Synergy HT (Bio Tek, Japan). The RT master mix was PrimeScript™ RT reagent Kit with gDNA Eraser (Takara bio, Japan), RNA content for RT was 300 ng, the PCR master mix was TB Green™ Premix Ex Taq™ II (Takara bio) and the real time PCR instrument was TP850 (Takara bio).

Primer sequence were as follows: *Akt1*, forward: ATGAACGACGTA GCCATTGTG, reverse: TTGTAGCCAATAAAGGTGCCAT; *Akt2*, forward: ACGTGGTGAATACATCAAGACC, reverse: GCTACAGAGAAATTGTTCA GGGG; *Ncam1*, forward: ACCACCGTCACCACTAACTCT, reverse: TGG GGCAATACTGGAGGTCA; *Gli1*, forward: CCAAGCCAACTTTATGTCA GGG, reverse: AGCCCGCTTCTTTGTTAATTTGA; *Ptch1*, forward: AAA GAACTGCGGCAAGTTTTTG, reverse: CTTCTCCTATCTTCTGACGGGT; *Rps18*, forward: CATGCAGAACCCACGACAGTA, reverse: CCTCACGCA GCTTGTTGTCTA.

2.9. Statistical analyses and data presentation

Results are expressed as mean ± SD. Statistical tests were performed using factorial ANOVA or repeated measurements ANOVA followed by Tukey's post hoc test where appropriate using SPSS 25 and GraphPad Prism 7. In cases where the data could not pass Levene's equal variance test even after transformations, Mann-Whitney test, a nonparametric test, as indicated in the figure legend, was applied to evaluate effects of botox or insulin within sub-groups. The significance level was set at $p < .05$. Number of observations is given in the figure legend.

3. Results

3.1. Botox-treatment in mice reduced body and soleus muscle weight

Mice injected with a pre-determined botox dose lost weight acutely and stabilized at ~ 1-g lower body weight compared to saline-only injected mice for the remainder of the 3-week study period (botox x time interaction, Fig. 1A). The data in Fig. 1 were compiled from several independent pilot-experiments in addition to the main experiment, accounting for the greater number of observations. At day 1 post-injection, the weight of the SO L muscle was not different when comparing botox-injected mice (contralateral and botox) to mice receiving saline injection in both legs (Fig. 1B). At day 21 post-injection, the weight of SOL muscle from saline-only injected mice was not different from the saline-injected soleus muscle from botox injected mice. In contrast, the botox-injected SOL exhibited significant atrophy in relation to both the contralateral soleus from the same mice and mice receiving saline only, weighing ~4 mg less (Fig. 1B). Since systemic botox spillover and functional overload of the contralateral leg might have affected our endpoints, we chose in the remaining analyses to use muscles from the separate mice receiving saline-only as controls for the botox-injected muscle, instead of the contralateral leg.

3.2. Insulin signaling and glucose handling proteins are dysregulated 21 days after botox treatment

No acute changes were observed on any total protein or phosphorylation measured on day 1 after botox-treatment (Fig. 2). In contrast, pronounced botox effects were observed after 21 days as described below (Fig. 3).

Glucose uptake is governed by GLUT4 dependent transport across the sarcolemma and T-tubular surface membranes followed by conversion into glucose-6-phosphate by HKII and both proteins are increased by exercise training and decreased by immobilization [35–37]. Here, both proteins exhibited ~60% lower expression in botox vs. saline-only muscles at day 21 (Figs. 3A + B).

Insulin-stimulated glucose transport into skeletal muscle requires the activation of the classical insulin signaling node Akt2, and denervation was previously shown to affect Akt2 expression and phosphorylation [10,12,15,16]. Insulin-stimulated Akt Ser473 and Thr308 phosphorylation were markedly higher at day 21 in botox vs. saline-treated muscle (Fig. 3C + D). The total protein expression of Akt2 was ~4-fold higher in botox vs. saline-only muscles at day 21 (Fig. 3E). The increases in Akt phosphorylation were lost when normalizing to total Akt protein (Fig. 3F + G), suggesting that the increased Akt phosphorylations may be caused by the increased protein expression.

TBC1D4 is phosphorylated by Akt2 to stimulate GLUT4 translocation in adipose and muscle cells [38–40]. Interestingly, despite the increased Akt phosphorylation, TBC1D4 Thr642 phosphorylation (Fig. 3H) and total protein (Fig. 3I) were strikingly lowered to ~20–30% of saline-control levels at day 21. This difference persisted after normalization for total protein (Fig. 3J), suggesting that botox affects the ability for Akt to signal to TBC1D4 at day 21. Among stress-induced phospho-proteins, ACC total was significantly lower and ACC Ser212/total protein significantly higher in botox-treated muscles after 21 days (Fig. 3K–M). Phosphorylation of p38 MAPK was unaltered by botox treatment (Fig. 3O).

3.3. Maximal insulin-stimulated glucose transport is not reduced by chemical denervation

Based on previous studies [10–14], we anticipated that chemical denervation by botox might acutely reduce insulin-stimulated glucose transport in skeletal muscle. In particular, we hypothesized that the reductions in GLUT4 and HKII would decrease the maximal insulin-stimulated capacity for glucose transport. To test this, we compared maximal insulin-stimulated 2DG transport in saline vs. botox-injected muscles. At day 1, 7 and 21, insulin increased glucose transport similarly in muscles receiving saline-only and botox (Fig. 4). Thus, despite the lower GLUT4 and HKII protein expression and the altered Akt-signaling, the maximal capacity for insulin-stimulated glucose transport was unaltered.

3.4. Submaximal insulin-stimulated TBC1D4 signaling and glucose transport were reduced by chemical denervation

Global KO of Akt2 in mice reduces submaximal, but not maximal insulin-stimulated glucose transport in isolated SOL and extensor digitorum longus (EDL) muscle [41]. We therefore performed a follow-up experiment looking at submaximal insulin-stimulated glucose transport and cell signaling in SOL ex vivo after 1 and 7 days of botox or saline-treatment. Given the marked effects on insulin-signaling, we also measured fasting glucose and insulin and calculated the HOMA2-IR. Body weight showed a main effect of botox but this reflected a tendency

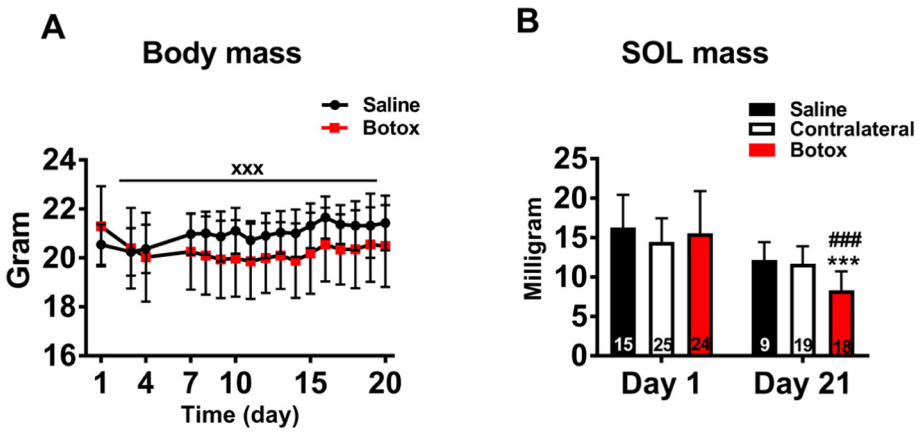

Fig. 1. Soleus (SOL) muscle mass decreased at day 21 post intramuscular botox injection.
A) Body mass of saline or botox injected mice was recorded for 20 days. xxx $p < .001$ interaction effect (botox x time). N = 10 and 18 for saline and botox group, respectively. B) Weight of SOL at 1 and 21 days after botox-treatment. The number of observations is indicated on the bars. ***/### $p < .001$ vs. saline/contralateral in Day 21 group. Data are expressed as mean ± SD.

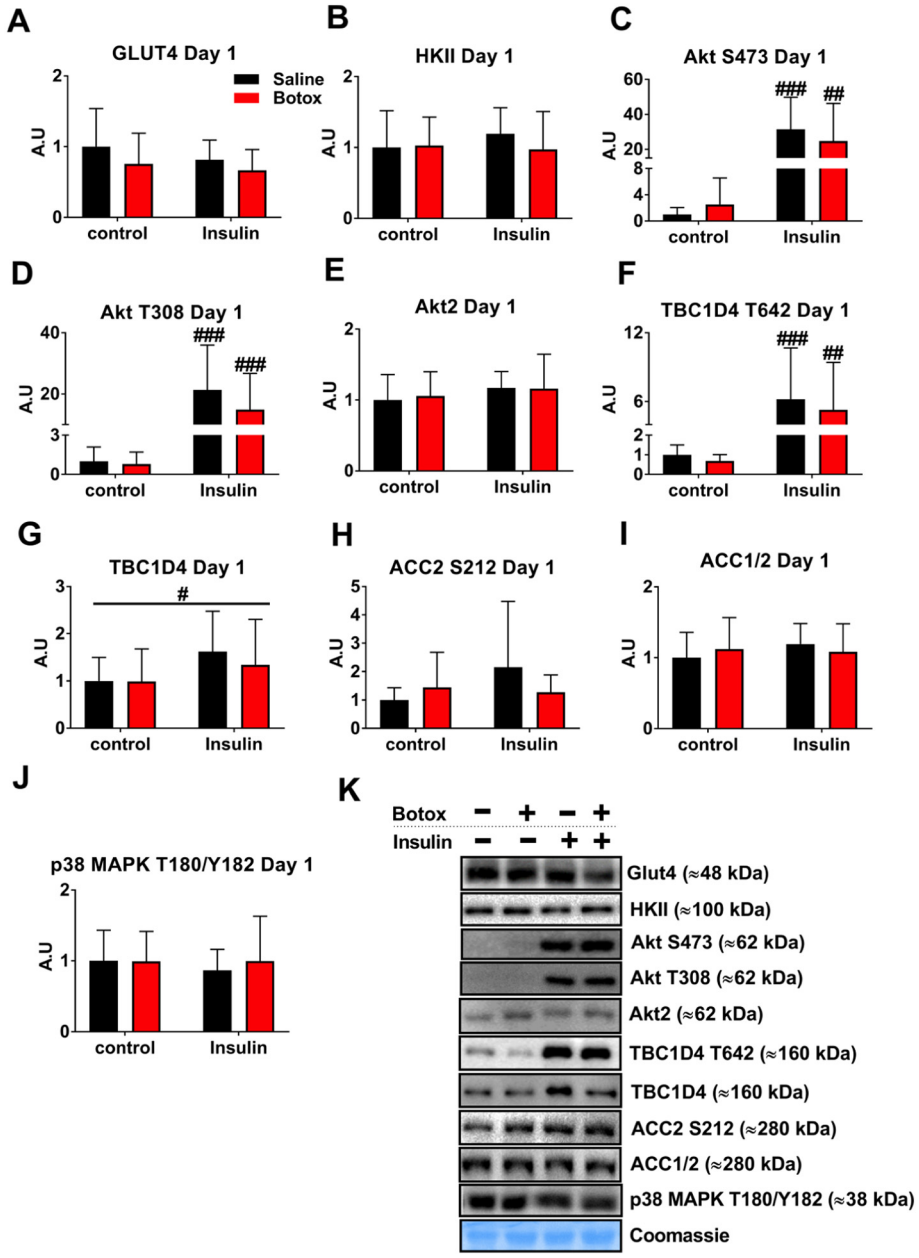

Fig. 2. Neither total protein nor insulin responsiveness changed in soleus (SOL) muscle at day 1 post botox injection.
A–J) Protein expression and phosphorylation level of SOL muscle incubated ± 60 nM insulin for 20 min were determined by western blotting. The color legend in A is shared with B-J. The proteins and phosphorylated proteins measured were: GLUT4, HKII, Akt Ser473, Akt Thr308, Akt2, TBC1D4 Thr642, TBC1D4, ACC2 Ser212, ACC1/2 total, p38 MAPK Thr180/Tyr182. For C, D & F), Mann-Whitney test, a nonparametric test, was applied to evaluate effect of insulin within saline or botox treated subgroups. ##, ### $p < .01$, 0.001. For G), # $p < .05$, insulin main effect. K) Representative blots for A–J. Coomassie stained membrane was used as loading control. Data are expressed as mean ± SD. n = 10–12.

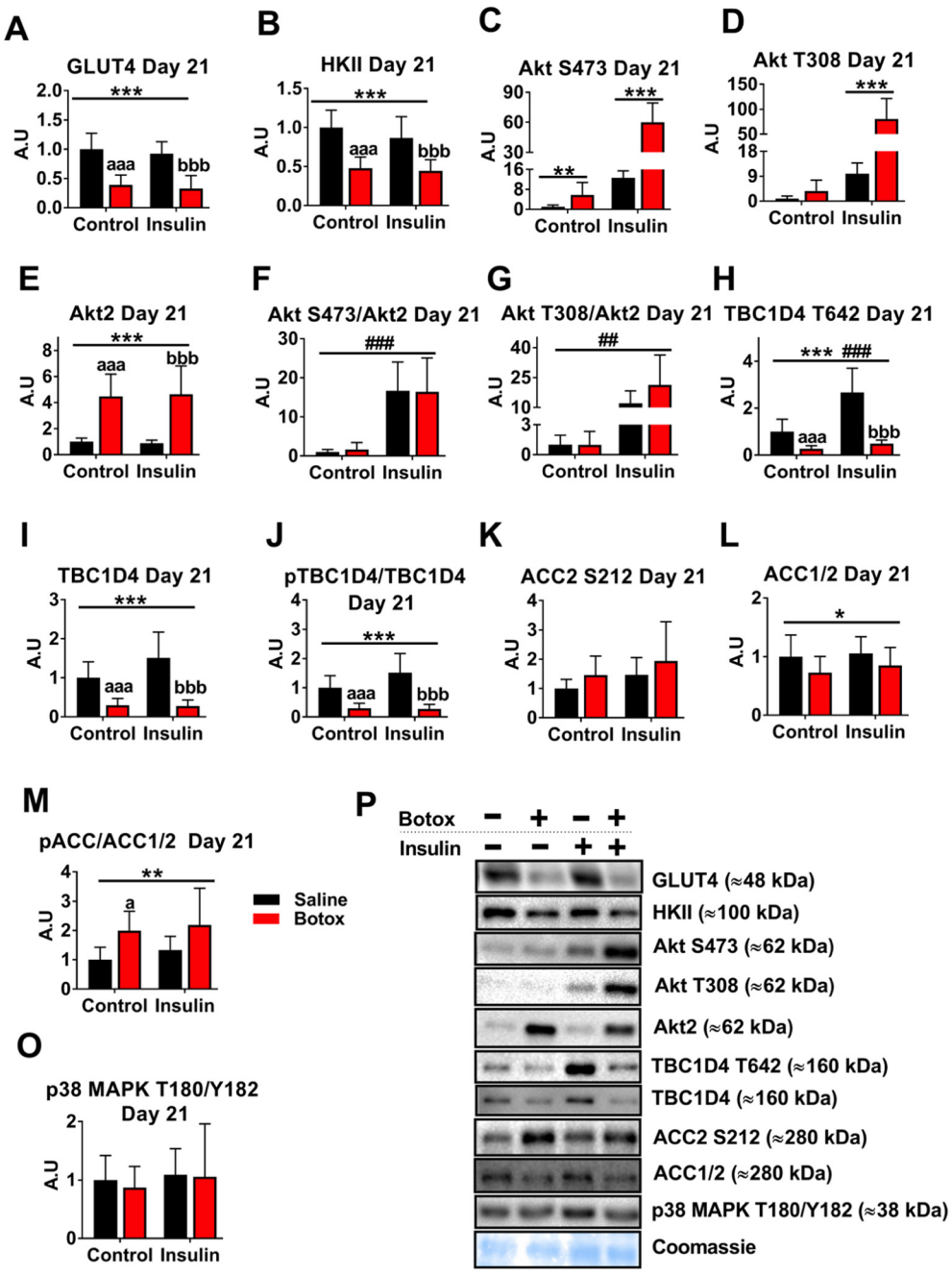

Fig. 3. Marked changes occur in total protein and insulin-responsiveness in soleus (SOL) muscle at day 21 post botox injection. A–J) Protein expression and phosphorylation level of SOL muscle incubated ± 60 nM insulin for 20 min were determined by western blotting. The color legend in M is shared with A-O. The proteins and phosphorylated proteins studied were: GLUT4, HKII, Akt Ser473, Akt Thr308, Akt2, TBC1D4 Thr642, TBC1D4, ACC2 Ser212, ACC1/2 total and p38 MAPK Thr180/Tyr182 (A-E, H, I, K, L & O). For A, B, E, F, H-J, L and M, *, **, *** $p < .05$, 0.01, 0.001 botox main effect. ### $p < .001$ insulin main effect. a, aaa $p < .05$, 0.001 vs. non-insulin and non-botox treated muscle. bbb $p < .001$ vs. insulin but non-botox treated muscle. For C, D and G, Mann-Whitney test, a nonparametric test, was applied to evaluate effect of botox within control or insulin treated subgroups. **, *** $p < .01$, 0.001. P) Representative blots for A–O. Coomassie stained membrane was used as loading control. Data are expressed as mean ± SD. n = 7–10.

towards a baseline difference and an increase in body weight in the saline-group rather than a decrease in the botox-group (Fig. 5A). Food intake was not different (Fig. 5B). Fasting glucose (Fig. 5C) and insulin (Fig. 5D) measured immediately post-mortem and the derived HOMA2-IR (Fig. 5E) were on average slightly higher in the botox groups but this was not significant. Submaximal insulin-stimulated glucose transport was significantly reduced at day 1 and showed a tendency to be reduced at day 7 (Fig. 5F). Akt expression, Thr308 and Ser473 phosphorylation were increased and TBC1D4 expression and Thr642 phosphorylation and GLUT4 were reduced at day 7 after botox-treatment (Fig. 6A–F). Unlike at 21 days, HKII was not reduced at 7 days (Fig. 6G). ACC2 Ser212 was significantly increased at 7 days with no change in total ACC protein expression (Fig. 6H–I).

3.5. Increased Akt protein is likely explained by increased mRNA expression but likely independent of the Hedgehog pathway

Gastrocnemius muscle was collected at day 7 to verify atrophy of the botox-treated muscle fibers and to perform PCR analyses. Fiber cross-sectional area was significantly reduced by approximately 50% at 7 days after botox-treatment compared to the saline control (Fig. 7A–B). Furthermore, Akt2 protein expression was greatly increased at day 7 (Fig. 7C). *Akt1* and, to a lesser extent, *Akt2* mRNA were also increased at day 7 but not day 1 after botox (Fig. 7D–E). Consistent with denervation, the denervation marker *Ncam1* was also upregulated at day 7 (Fig. 7F). We hypothesized the increased Akt mRNA expression to be driven by increased Hedgehog signaling but found the two Hedgehog-signaling pathway regulated genes, *Gli1* and *Ptch1*, not to be increased by botox (Fig. 7G–H).

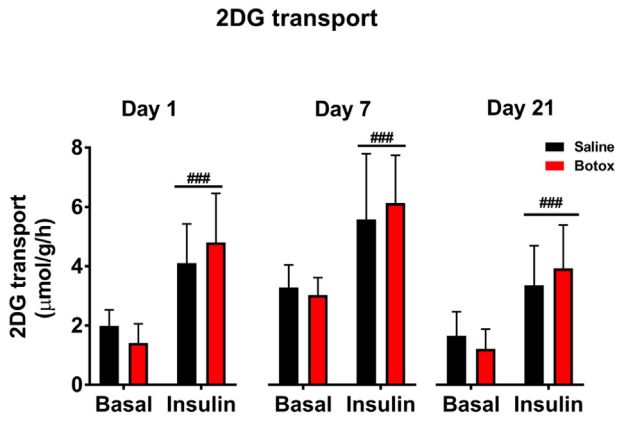

Fig. 4. Maximal insulin-stimulated glucose transport was not affected by botox injection in soleus (SOL) muscle.
Insulin stimulated 2-deoxy glucose (2DG) transport (60 nM, 2DG tracer last 10 min of 20 min insulin-stimulation, 1 and 21 days are the same muscles as in Fig. 2+3) in ex vivo incubated SOL was assessed 1 day, day 7 or 21 days post botox-injection. ### $p < .001$ insulin main effect. Significance level was set to 0.05. Data are expressed as mean ± SD. n = 7–10.

4. Discussion

We currently tested the impact of chemical denervation by botox on insulin signaling and glucose transport in mouse muscle. Botox treatment decreased submaximal but not maximal insulin-stimulated glucose transport. Furthermore, botox profoundly influenced multiple steps of the insulin signaling cascade regulating GLUT4 translocation, in addition to the glucose handling machinery itself. Depending on the time point, botox-treatment increased Akt protein expression and phosphorylation, decreased TBC1D4 expression and phosphorylation and decreased GLUT4 and HKII expression. These changes demonstrate the scientific utility of botox-injection as a minimally invasive denervation model and suggest disturbed muscle insulin-signaling and glucose metabolism to be likely side-effects of clinical botox-treatment.

The reduced submaximal insulin-stimulated glucose transport in our study is in agreement with a another study which used unilateral surgical sciatic axotomy of mouse hind limbs and observed reduced glucose transport measured ex vivo after in vivo IP injection of insulin [16]. The reduction in submaximal and not maximal glucose transport may seem surprising given the alterations observed in Akt2 and the reductions observed in GLUT4 and HKII in botox-treated muscles. However, as stated reduced submaximal, but not maximal insulin-stimulated glucose transport ex vivo has been previously reported in Akt2 KO mice [41]. Similarly, muscle-specific disruption of the Akt Ser473 kinase complex mTORC2 by conditional KO of Rictor does not reduce maximal insulin-stimulated glucose transport ex vivo despite abolishing insulin-stimulated Akt Ser473 phosphorylation (Maximillian Kleinert and Erik Richter – unpublished data). Thus, insulin-stimulated Akt2 signaling may not be necessary for the glucose transport in response to a maximal insulin dose ex vivo. As for GLUT4, these data would suggest that a ~60% reduction in GLUT4 protein does not influence the maximal capacity for insulin-stimulated glucose transport ex vivo, either because the remaining ~40% of GLUT4 is sufficient to facilitate maximal glucose transport or because other transporter proteins are involved, as suggested recently for synergist ablation overload-induced glucose uptake [42]. As for HKII, this protein may be less critical to glucose uptake ex vivo, where transport rather than phosphorylation by HKII is proposed to be rate-limiting for insulin-stimulated glucose transport [43].

Increased Akt2 expression has been reported previously in the context of surgical denervation. Hence, recent rodent studies using unilateral mouse hind limb surgical denervation found Akt2 protein expression to be stably increased by ~40% from day 3 to 2 months after

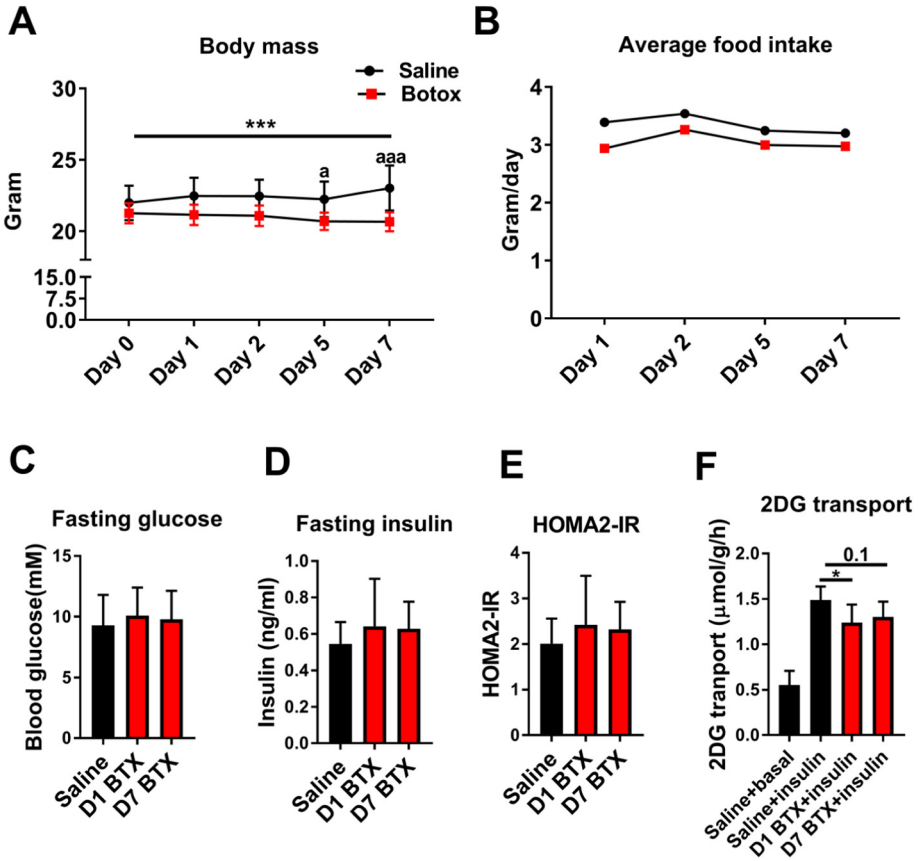

Fig. 5. Submaximal insulin-stimulated glucose transport was reduced by botox injection in soleus (SOL) muscle. A & B) Individual body mass and food intake per cage measured as indicated during the experimental period. The color legend in A) is shared with B). C-E) Fasting glucose, fasting insulin and HOMA2-IR index derived from C &D. F) Submaximal insulin stimulated 2-deoxy glucose (2DG) transport (1.5 nM, 2DG tracer last 10 min of 20 min insulin-stimulation) in ex vivo incubated SOL was assessed 1 day or 7 days post botox injection. For A), *** $p < .001$ Botox main effect; a $p < .05$ at given day. For F, only the insulin-stimulated groups were considered in the statistical analysis. * $p < .05$ vs saline + insulin; number stated above given bars indicates a tendency towards significance. D, day. BTX, Botox. Data are expressed as mean ± SD. n = 8.

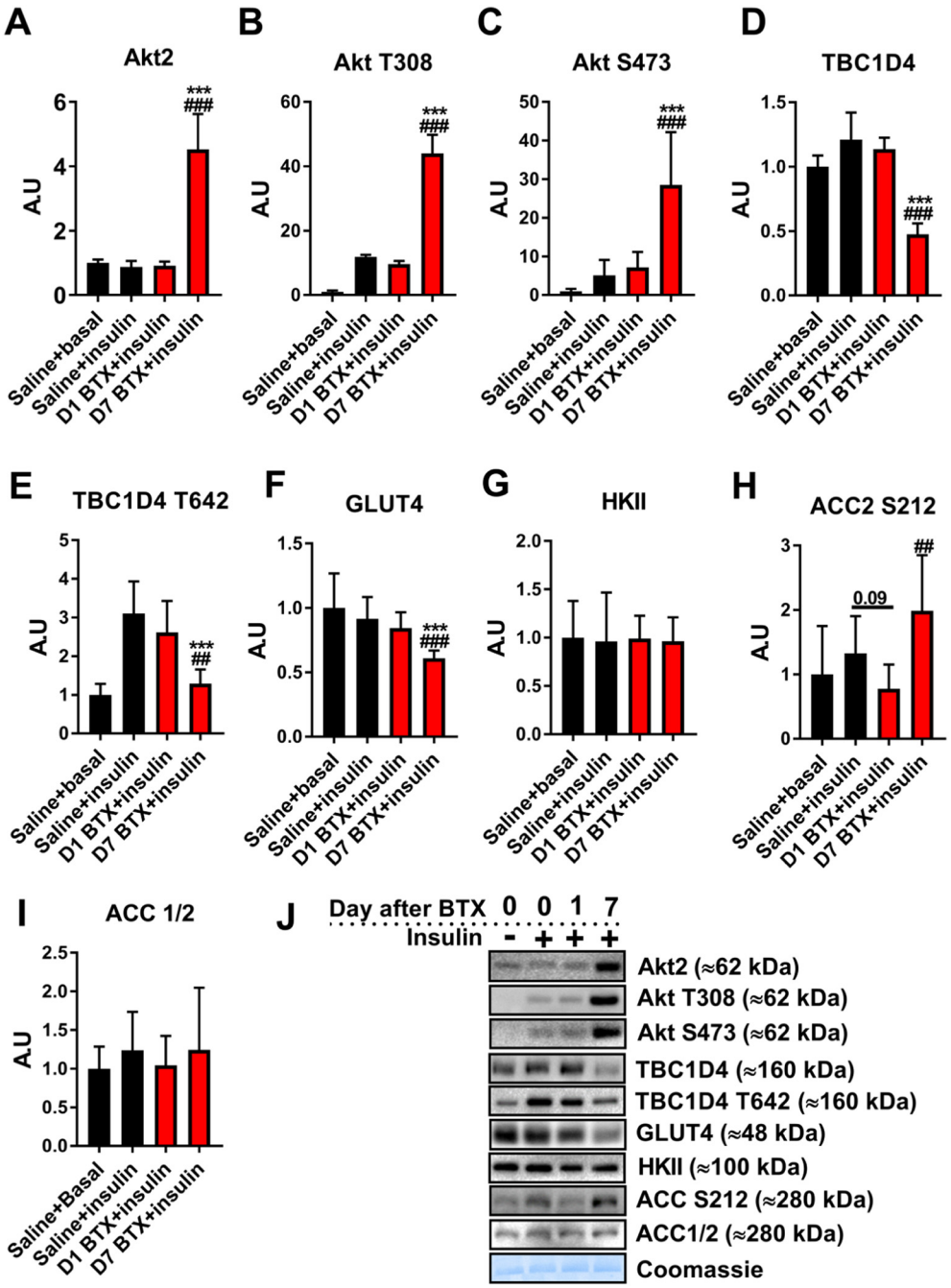

Fig. 6. Marked changes occurred in total protein and submaximal insulin signaling in soleus (SOL) muscle at day 7 post botox injection.

A–I) Protein expression and phosphorylation level of SOL muscle incubated ± 1.8 nM insulin for 20 min (the same muscles used in Fig. 5 F) were determined by western blotting. The proteins and phosphorylated proteins studied were: Akt2, Akt Thr308, Akt Ser473, TBC1D4, TBC1D4 Thr642, GLUT4, HKII, ACC2 Ser212 and ACC1/2 total. For A-I, only the insulin-stimulated groups were considered in the statistical analysis. *** $p < .001$ vs. saline + insulin. ##, ### $p < .01$, 0.001 vs. D1 BTX + insulin. Number stated above given bars indicates a tendency towards significance. D, day. BTX, Botox. J) Representative blots for A–I. Coomassie stained membrane was used as loading control. Data are expressed as mean ± SD. n = 8.

denervation and onwards in one study [16] and ~11-fold at 3 weeks after denervation [19]. Interestingly, the increase in Akt protein was only observed in mouse TA with denervation and not forced immobilization by surgical stapling [19], suggesting that the increased Akt expression does not relate to the functional muscle activity, but rather to the lack of neural innervation. Consistent with the notion that muscle activity does not regulate Akt2 protein expression, Akt2 protein expression is generally minimally responsive to various modes of exercise training in rodents [44–47] or humans [48,49].

The actual mechanism behind the increased Akt expression is unknown. Akt is frequently hyper-activated in cancer cells and transcription of the 3 distinct genes for Akt isoforms 1–3 appears to be coordinately regulated by the Hedgehog signaling and the transcriptional activator GLI1 [50]. Interestingly, Hedgehog signaling in cell-surface emanating organelles termed primary cilia was transiently up-regulated during myogenesis and necessary for differentiation of C2C12 mouse myoblasts [51]. Thus, we hypothesized that the currently observed increase in Akt protein might be part of a Hedgehog signaling-dependent myogenesis response. However, our mRNA data do not support this conclusion (Fig. 7E–F). It is worth noting that Akt1 and Akt2 KO both display reduced cross-sectional area in fast-twitch glycolytic EDL muscle, but that neither model shows reduced cross-sectional area in slow-twitch oxidative SOL muscle [52]. The absent phenotype could indicate that Akt is not essential to development and growth of SOL muscle. On the other hand, regeneration of adult muscle may be different. Degradation of Akt is also highly regulated by multiple mechanisms including the ubiquitin-proteasome pathway and caspase-mediated cleavage [53] which could contribute to the increased Akt protein.

A significant decrease in total body weight was observed in the botox-injected mice compared to the saline-only injected mice, in particular in our initial study injecting botox into both TA and triceps

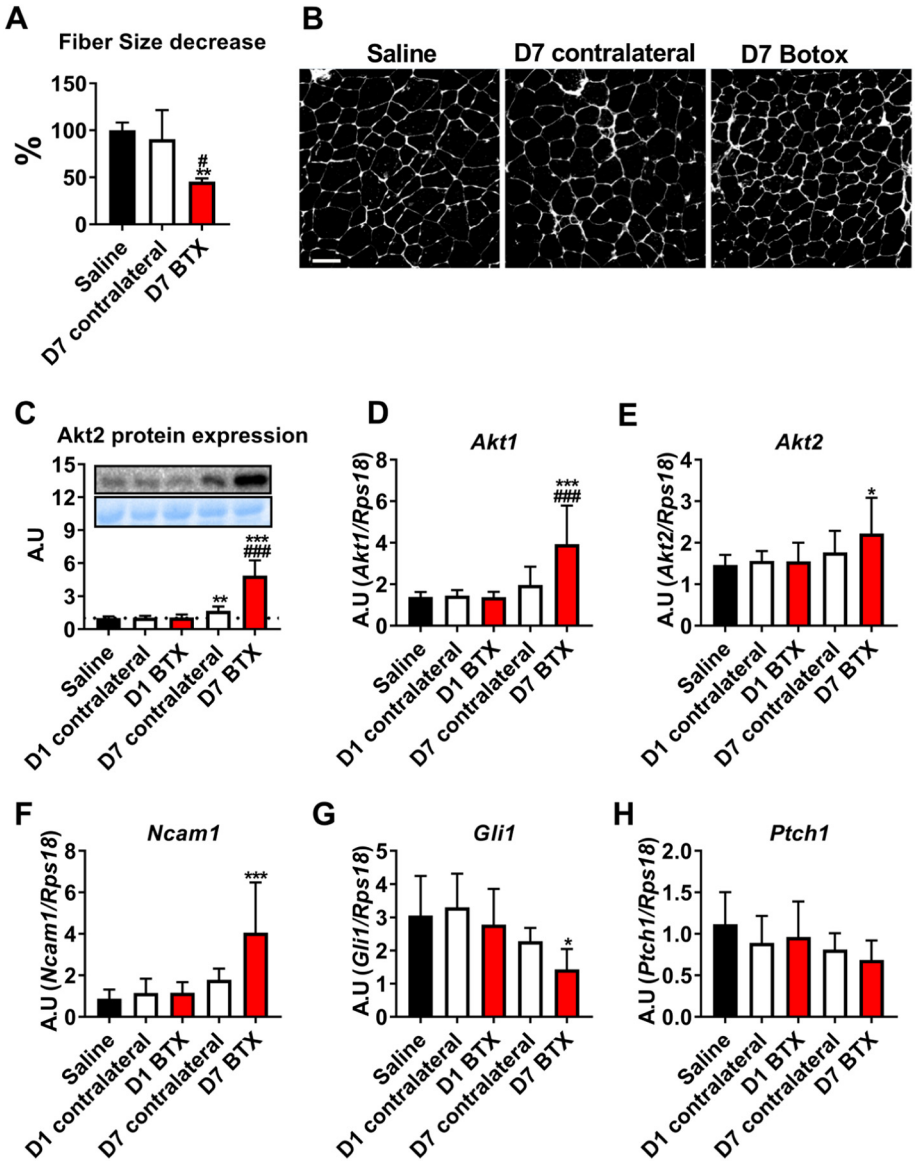

Fig. 7. Gastrocnemius muscles fiber size and mRNA expression profile were affected at day 7 post Botox injection.
A & B) Cross sectional area of gastrocnemius muscle fiber and representative images. Scale bar = 50 μm. N = 5–6. C–H) Gastrocnemius muscles were used to study protein expression of Akt2 and mRNA expression of *Akt1*, *Akt2*, *Ncam1*, *Gli1 and Ptch1*. For A, C–H, *, **, *** $p < .05, 0.01, 0.001$ vs. saline; #, ### $p < .05, 0.001$ vs. D7 contralateral. N = 7–8. D, day. BTX, Botox. Data are expressed as mean ± SD.

surae. This is supported by earlier findings of weight loss after injection in mice with the same dosage of botox as our study, with a peak after 14 days, which then reverted to the normal weight after 21 days [24]. In contrast, no body weight difference was found between mice injected with half the dosage of botox compared to saline injected mice [54]. This is also consistent with the absence of decreased body weight in our follow-up study injecting triceps surae only (i.e. half the dosage). To our knowledge, no human studies have reported body weight loss as a side effect of botox treatment. Although the initially used dosage was based on previous studies in mice, the negative effect of botox-treatment on body weight in mice is likely reflective of over-dosing. We fully acknowledge this limitation in our experimental setup and do not recommend a 1 U total botox dosage for future chemical denervation experiments. Nonetheless, only the botox-treated SOL muscle, but not the contralateral leg, was reduced in mass compared to the saline control, suggesting that the loss of muscle mass resulted predominantly from the chemical denervation and not from general loss of body mass.

In summary, chemical denervation by local botox injection elicits a phenotype reminiscent of surgical denervation with marked muscle atrophy. This was accompanied by increased Akt expression and phosphorylation and, depending on the time-point, reduced expression of muscle activity-dependent proteins such as GLUT4 and HKII and phosphorylation and expression of the GLUT4 translocation-regulating TBC1D4 protein. Importantly, botox-induced insulin resistance was evident at submaximal but not maximal insulin concentration ex vivo. The marked alterations in Akt-TBC1D4 signaling, GLUT4 and HKII and glucose transport are potential concerns with botox treatment which warrant further investigation in mice and humans.

Conflict of interest

Zhencheng Li, Lui Näslund-Koch, Carlos Henriquez Olguin, Jonas Roland Knudsen, Jingwen Li, Agnete B. Madsen, Saturo Ato, Jacob Wienecke, Riki Ogasawara, Jens B. Nielsen and Thomas E. Jensen declare that they have no conflict of interest.

Author contributions

TEJ, JBN and JW conceived the study. ZL, LNK, JBN, CHO, JL, ABM, JRK and TEJ performed the experiments. ZL and LNK performed the biochemical analyses. JRK measured fiber-size. SA and RO performed PCR. JW applied for ethical approval. LNK, ZL and TEJ wrote the manuscript with input from all co-authors. All authors approved the final version of the manuscript.

Acknowledgements

This study was supported by a Novo Nordisk Foundation Excellence project grant (#15182) to TEJ, a Danish Research Council grant (4183-00462B) to JBN and JW, China Scholarship Council (CSC) Ph.D. stipends to ZL and JL, Danish Diabetes Academy PhD stipends to ABM and JRK and a Chilean National Commission for Scientific and Technological Research (CONICYT) Ph.D. Scholarship to CHO.

References

[1] M. Hallett, A. Albanese, D. Dressler, K.R. Segal, D.M. Simpson, D. Truong, et al., Evidence-based review and assessment of botulinum neurotoxin for the treatment of movement disorders, Toxicon 67 (2013 Jun 1) 94–114.
[2] T. Rekand, Clinical assessment and management of spasticity: a review, Acta Neurol. Scand. Suppl. 190 (2010) 62–66.
[3] H.K. Graham, K.R. Aoki, I. Autti-Ramo, R.N. Boyd, M.R. Delgado, D.J. Gaebler-Spira, et al., Recommendations for the use of botulinum toxin type A in the management of cerebral palsy, Gait Posture 11 (1) (2000 Feb) 67–79.
[4] S. Xue, S. Javor, M.S. Hixon, K.D. Janda, Probing BoNT/a protease exosites: implications for inhibitor design and light chain longevity, Biochemistry 53 (43) (2014 Nov 4) 6820–6824.
[5] J. Blasi, E.R. Chapman, E. Link, T. Binz, S. Yamasaki, C.P. De, et al., Botulinum neurotoxin a selectively cleaves the synaptic protein SNAP-25, Nature 365 (6442) (1993 Sep 9) 160–163.
[6] G.E. Borodic, R. Ferrante, L.B. Pearce, K. Smith, Histologic assessment of dose-related diffusion and muscle fiber response after therapeutic botulinum a toxin injections, Mov. Disord. 9 (1) (1994 Jan) 31–39.
[7] B. Mohammadi, S.A. Balouch, R. Dengler, K. Kollewe, Long-term treatment of spasticity with botulinum toxin type A: an analysis of 1221 treatments in 137 patients, Neurol. Res. 32 (3) (2010 Apr) 309–313.
[8] J. Pingel, M.S. Nielsen, T. Lauridsen, K. Rix, M. Bech, T. Alkjaer, et al., Injection of high dose botulinum-toxin A leads to impaired skeletal muscle function and damage of the fibrilar and non-fibrilar structures, Sci. Rep. 7 (1) (2017 Nov 7) 14746.
[9] K. Mukund, M. Mathewson, V. Minamoto, S.R. Ward, S. Subramaniam, R.L. Lieber, Systems analysis of transcriptional data provides insights into muscle's biological response to botulinum toxin, Muscle Nerve 50 (5) (2014 Nov) 744–758.
[10] N.E. Block, D.R. Menick, K.A. Robinson, M.G. Buse, Effect of denervation on the expression of two glucose transporter isoforms in rat hindlimb muscle, J. Clin. Invest. 88 (5) (1991 Nov) 1546–1552.
[11] E.J. Henriksen, M.E. Tischler, Glucose uptake in rat soleus: effect of acute unloading and subsequent reloading, J. Appl. Physiol. 64 (4) (1988 Apr) 1428–1432.
[12] E.J. Henriksen, K.J. Rodnick, C.E. Mondon, D.E. James, J.O. Holloszy, Effect of denervation or unweighting on GLUT-4 protein in rat soleus muscle, J. Appl. Physiol. 70 (5) (1991 May) 2322–2327.
[13] J. Lin, P.H. Wu, P.T. Tarr, K.S. Lindenberg, J. St-Pierre, C.Y. Zhang, et al., Defects in adaptive energy metabolism with CNS-linked hyperactivity in PGC-1alpha null mice, Cell 119 (1) (2004 Oct 1) 121–135.
[14] D.B. Thomason, R.E. Herrick, D. Surdyka, K.M. Baldwin, Time course of soleus muscle myosin expression during hindlimb suspension and recovery, J. Appl. Physiol. 63 (1) (1987 Jul) 130–137.
[15] R.B. Didyk, E.E. Anton, K.A. Robinson, D.R. Menick, M.G. Buse, Effect of immobilization on glucose transporter expression in rat hindlimb muscles, Metabolism 43 (11) (1994 Nov) 1389–1394.
[16] Z.J. Callahan, M. Oxendine, J.L. Wheatley, C. Menke, E.A. Cassell, A. Bartos, et al., Compensatory responses of the insulin signaling pathway restore muscle glucose uptake following long-term denervation, Physiol. Rep. 3 (4) (2015 Apr).
[17] L.A. Megeney, R.N. Michel, C.S. Boudreau, P.K. Fernando, M. Prasad, M.H. Tan, et al., Regulation of muscle glucose transport and GLUT-4 by nerve-derived factors and activity-related processes, Am. J. Phys. 269 (5 Pt 2) (1995 Nov) R1148–R1153.
[18] L. Coderre, M.M. Monfar, K.S. Chen, S.J. Heydrick, T.G. Kurowski, N.B. Ruderman, et al., Alteration in the expression of GLUT-1 and GLUT-4 protein and messenger RNA levels in denervated rat muscles, Endocrinology 131 (4) (1992 Oct) 1821–1825.
[19] E.M. MacDonald, E. Andres-Mateos, R. Mejias, J.L. Simmers, R. Mi, J.S. Park, et al., Denervation atrophy is independent from Akt and mTOR activation and is not rescued by myostatin inhibition, Dis. Model. Mech. 7 (4) (2014 Apr) 471–481.
[20] F. Lang, S. Aravamudhan, H. Nolte, C. Turk, S. Holper, S. Muller, et al., Dynamic changes in the mouse skeletal muscle proteome during denervation-induced atrophy, Dis. Model. Mech. 10 (7) (2017 Jul 1) 881–896.
[21] A.A. Rogozhin, K.K. Pang, E. Bukharaeva, C. Young, C.R. Slater, Recovery of mouse neuromuscular junctions from single and repeated injections of botulinum neurotoxin A, J. Physiol. 586 (13) (2008 Jul 1) 3163–3182.
[22] P.J. Niziolek, W. Bullock, M.L. Warman, A.G. Robling, Missense mutations in LRP5 associated with high bone mass protect the mouse skeleton from disuse- and ovariectomy-induced osteopenia, PLoS One 10 (11) (2015) e0140775.
[23] Y. Torii, Y. Goto, S. Nakahira, S. Kozaki, R. Kaji, A. Ginnaga, Comparison of systemic toxicity between botulinum toxin subtypes A1 and A2 in mice and rats, Basic Clin. Pharmacol. Toxicol. 116 (6) (2015 Jun) 524–528.
[24] S.E. Warner, D.A. Sanford, B.A. Becker, S.D. Bain, S. Srinivasan, T.S. Gross, Botox induced muscle paralysis rapidly degrades bone, Bone 38 (2) (2006 Feb) 257–264.
[25] T.D. Wilder-Kofie, C. Luquez, M. Adler, J.K. Dykes, J.D. Coleman, S.E. Maslanka, An alternative in vivo method to refine the mouse bioassay for botulinum toxin detection, Comp. Med. 61 (3) (2011 Jun) 235–242.
[26] S.J. Warden, M.R. Galley, J.S. Richard, L.A. George, R.C. Dirks, E.A. Guildenbecher, et al., Reduced gravitational loading does not account for the skeletal effect of botulinum toxin-induced muscle inhibition suggesting a direct effect of muscle on bone, Bone 54 (1) (2013 May) 98–105.
[27] C. Pehmoller, J.T. Treebak, J.B. Birk, S. Chen, C. Mackintosh, D.G. Hardie, et al., Genetic disruption of AMPK signaling abolishes both contraction- and insulin-stimulated TBC1D1 phosphorylation and 14-3-3 binding in mouse skeletal muscle, Am. J. Physiol. Endocrinol. Metab. 297 (3) (2009 Sep) E665–E675.
[28] R. Aslesen, J. Jensen, Effects of epinephrine on glucose metabolism in contracting rat skeletal muscles, Am. J. Phys. 275 (3 Pt 1) (1998 Sep) E448–E456.
[29] A.J. Kolnes, J.B. Birk, E. Eilertsen, J.T. Stuenaes, J.F. Wojtaszewski, J. Jensen, Epinephrine-stimulated glycogen breakdown activates glycogen synthase and increases insulin-stimulated glucose uptake in epitrochlearis muscles, Am. J. Physiol. Endocrinol. Metab. 308 (3) (2015 Feb 1) E231–E240.
[30] J. Buren, Y.C. Lai, M. Lundgren, J.W. Eriksson, J. Jensen, Insulin action and signalling in fat and muscle from dexamethasone-treated rats, Arch. Biochem. Biophys. 474 (1) (2008 Jun 1) 91–101.
[31] Z. Li, M.L. Rasmussen, J. Li, C.H. Olguin, J.R. Knudsen, O. Sogaard, et al., Low- and high-protein diets do not alter ex vivo insulin action in skeletal muscle, Physiol. Rep. 6 (13) (2018 Jul) e13798.
[32] J.F. Wojtaszewski, A.B. Jakobsen, T. Ploug, E.A. Richter, Perfused rat hindlimb is suitable for skeletal muscle glucose transport measurements, Am. J. Phys. 274 (1 Pt 1) (1998 Jan) E184–E191.
[33] T.E. Jensen, A.J. Rose, S.B. Jorgensen, N. Brandt, P. Schjerling, J.F. Wojtaszewski, et al., Possible CaMKK-dependent regulation of AMPK phosphorylation and glucose uptake at the onset of mild tetanic skeletal muscle contraction, Am. J. Physiol. Endocrinol. Metab. 292 (5) (2007 May) E1308–E1317.
[34] S. Ato, Y. Makanae, K. Kido, K. Sase, N. Yoshii, S. Fujita, The effect of different acute muscle contraction regimens on the expression of muscle proteolytic signaling proteins and genes, Physiol. Rep. 5 (15) (2017 Aug).
[35] R.S. Bienso, S. Ringholm, K. Kiilerich, N.J. Aachmann-Andersen, R. Krogh-Madsen, B. Guerra, et al., GLUT4 and glycogen synthase are key players in bed rest-induced insulin resistance, Diabetes 61 (5) (2012 May) 1090–1099.
[36] J.L. Andersen, P. Schjerling, L.L. Andersen, F. Dela, Resistance training and insulin action in humans: effects of de-training, J. Physiol. 551 (Pt 3) (2003 Sep 15) 1049–1058.
[37] A.C. Alibegovic, M.P. Sonne, L. Hojbjerre, J. Bork-Jensen, S. Jacobsen, E. Nilsson, et al., Insulin resistance induced by physical inactivity is associated with multiple transcriptional changes in skeletal muscle in young men, Am. J. Physiol. Endocrinol. Metab. 299 (5) (2010 Nov) E752–E763.
[38] G.D. Cartee, K. Funai, Exercise and insulin: Convergence or divergence at AS160 and TBC1D1? Exerc. Sport Sci. Rev. 37 (4) (2009 Oct) 188–195.
[39] S. Chen, D.H. Wasserman, C. Mackintosh, K. Sakamoto, Mice with AS160/TBC1D4-Thr649Ala knockin mutation are glucose intolerant with reduced insulin sensitivity and altered GLUT4 trafficking, Cell Metab. 13 (1) (2011 Jan 5) 68–79.
[40] C.P. Miinea, H. Sano, S. Kane, E. Sano, M. Fukuda, J. Peranen, et al., AS160, the Akt substrate regulating GLUT4 translocation, has a functional Rab GTPase-activating protein domain, Biochem. J. 391 (Pt 1) (2005 Oct 1) 87–93.
[41] H. Cho, J. Mu, J.K. Kim, J.L. Thorvaldsen, Q. Chu, E.B. Crenshaw IIIet al., Insulin resistance and a diabetes mellitus-like syndrome in mice lacking the protein kinase Akt2 (PKB beta), Science 292 (5522) (2001 Jun 1) 1728–1731.
[42] S.L. McMillin, D.L. Schmidt, B.B. Kahn, C.A. Witczak, GLUT4 is not necessary for overload-induced glucose uptake or hypertrophic growth in mouse skeletal muscle, Diabetes 66 (6) (2017 Jun) 1491–1500.
[43] P.A. Hansen, B.A. Marshall, M. Chen, J.O. Holloszy, M. Mueckler, Transgenic overexpression of hexokinase II in skeletal muscle does not increase glucose disposal in wild-type or Glut1-overexpressing mice, J. Biol. Chem. 275 (29) (2000 Jul 21) 22381–22386.
[44] S. Cao, B. Li, X. Yi, B. Chang, B. Zhu, Z. Lian, et al., Effects of exercise on AMPK signaling and downstream components to PI3K in rat with type 2 diabetes, PLoS One 7 (12) (2012) e51709.
[45] A.D. Krisan, D.E. Collins, A.M. Crain, C.C. Kwong, M.K. Singh, J.R. Bernard, et al., Resistance training enhances components of the insulin signaling cascade in normal and high-fat-fed rodent skeletal muscle, J. Appl. Physiol. 96 (5) (2004 May) 1691–1700.
[46] R. Marinho, L.P. Moura, B.A. Rodrigues, L.S. Pauli, A.S. Silva, E.C. Ropelle, et al., Effects of different intensities of physical exercise on insulin sensitivity and protein kinase B/Akt activity in skeletal muscle of obese mice, Einstein (Sao Paulo) 12 (1) (2014 Jan) 82–89.
[47] B.B. Yaspelkis III, S.J. Lessard, D.W. Reeder, J.J. Limon, M. Saito, D.A. Rivas, et al., Exercise reverses high-fat diet-induced impairments on compartmentalization and activation of components of the insulin-signaling cascade in skeletal muscle, Am. J. Physiol. Endocrinol. Metab. 293 (4) (2007 Oct) E941–E949.

[48] T.R. Andersen, J.F. Schmidt, M.T. Pedersen, P. Krustrup, J. Bangsbo, The effects of 52 weeks of soccer or resistance training on body composition and muscle function in +65-year-old healthy males - a randomized controlled trial, PLoS One 11 (2) (2016) e0148236.

[49] C. Frosig, A.J. Rose, J.T. Treebak, B. Kiens, E.A. Richter, J.F. Wojtaszewski, Effects of endurance exercise training on insulin signaling in human skeletal muscle: interactions at the level of phosphatidylinositol 3-kinase, Akt, and AS160, Diabetes 56 (8) (2007 Aug) 2093–2102.

[50] N.K. Agarwal, C. Qu, K. Kunkalla, Y. Liu, F. Vega, Transcriptional regulation of serine/threonine protein kinase (AKT) genes by glioma-associated oncogene homolog 1, J. Biol. Chem. 288 (21) (2013 May 24) 15390–15401.

[51] W. Fu, P. Asp, B. Canter, B.D. Dynlacht, Primary cilia control hedgehog signaling during muscle differentiation and are deregulated in rhabdomyosarcoma, Proc. Natl. Acad. Sci. U. S. A. 111 (25) (2014 Jun 24) 9151–9156.

[52] M.D. Goncalves, E.E. Pistilli, A. Balduzzi, M.J. Birnbaum, J. Lachey, T.S. Khurana, et al., Akt deficiency attenuates muscle size and function but not the response to ActRIIB inhibition, PLoS One 5 (9) (2010) e12707.

[53] Y. Liao, M.C. Hung, Physiological regulation of Akt activity and stability, Am. J. Transl. Res. 2 (1) (2010) 19–42.

[54] S.L. Manske, S.K. Boyd, R.F. Zernicke, Muscle and bone follow similar temporal patterns of recovery from muscle-induced disuse due to botulinum toxin injection, Bone 46 (1) (2010 Jan) 24–31.